

BUILDING APPENDAGE SEISMIC DESIGN FORCE
BASED ON OBSERVED FLOOR RESPONSE

Yuji Sato (I)
Tatsuro Fuse (II)
Hisanobu Akagi (III)
Presenting Author: H. Akagi

SUMMARY

NTT has installed SMAC type strong-motion accelerographs in a number of selected buildings owned by NTT and carried out earthquake observation since 1960. The authors analyzed the data gained through the observation, particularly with respect to comparatively heavy earthquakes, and proposed a method for calculating the seismic forces data used for designing an appendage to the building, based upon the analysis result.

1. INTRODUCTION

In order to reasonably conduct aseismic designing for so-called appendages, such as various structures and non-structural components that are attached to the buildings, equipments and fixtures that are contained therein and their supporting and connecting parts, the design should be based upon the concept that has been systematized as a combined system of building-appendages, in which the seismic motion transmission process is taken into consideration. In doing so, after the building and the specific floor etc. to which the appendage is installed has been determined, the seismic force estimation method for designing could be worked out from the building and appendages vibration characteristics. However, when the building cannot be specified, for instance, in case the equipment or construction elements available on the market are to be developed, if the aseismic designing is done by assuming the vibration characteristics of the building that would induce the highest acceleration response to the appendages, the result would probably be surplus strength for most of the appendages. Therefore, investigation must be made on an adequate level of the seismic force data to be assumed for designing.

In this study, the authors gained knowledge concerning the natural vibration period of buildings, the acceleration amplification ratios along the height direction of the building, the acceleration response spectra of the building floor etc. by analyzing the earthquake observation records collected from the "SMAC" type strong-motion accelerographs installed in NTT buildings. Besides, they investigated the seismic

-
- (I) Chief of Structural Engineering Section, Musashino Electrical Communication Laboratory, Nippon Telegraph and Telephone Public Corporation, Tokyo, JAPAN
 - (II) Staff Engineer, Building Bureau, NTT., Tokyo, JAPAN
 - (III) Assistant Chief of Structural Engineering Section, MECL., NTT., Tokyo, JAPAN

force to be assumed when the appendages to the building are designed and undertook to make a proposal concerning the calculation method.

2. INSTALLATION OF STRONG-MOTION ACCELEROGRAPHS

The first strong-motion accelerograph in NTT was installed in 1960. The number of installations has increased up to 107 sets as of the end of 1981, distributed in buildings at 41 locations, most of them telephone exchanges, all over Japan. Up to now, the seismic wave records for more than 1,300 have been recorded. Figure 1 shows the installation layout for strongmotion accelerographs in Izu Itoh Exchange as an example and some samples of the seismic waveforms obtained by them are shown.

The structural characteristics of buildings in which the strong-motion accelerographs are installed are as mentioned below. Most of them are telephone exchanges and include exchange equipment rooms with large floor to floor height and heavy loading.

- (1) If classified by structure, buildings 5 stories high and higher are steel skeleton and reinforced concrete construction (SRC). Most buildings 4 stories high and lower are reinforced concrete construction (RC). The wall length is large, its value is around 5 cm/m^2 in most of the buildings.
- (2) The majority of the buildings have 2 to 10 stories aboveground. About half of them have 4 to 6 stories. More than half of the buildings have from 1 to 4 basements.
- (3) The floor height ranges from 4.2 to 5 meters for equipment rooms and is around 3.6 meters for the offices. About half of the buildings have either uneven floor height or skipped floor construction, because the equipment rooms and the office spaces are arranged mixed in these buildings.

As installation locations for the strong-motion accelerographs, the bottom floor, and the roof or the uppermost floor were chosen in principle. In some buildings, 1 ~ 3 additional instruments were installed on intermediate stories.

The number of stories, the construction, the soil and the foundation for the buildings in which the strong-motion accelerographs are installed and the floors where the accelerograph is installed are summarized in Fig. 2.

3. OUTLINE OF DATA OBSERVED AND ANALYSIS METHOD

The maximum acceleration of seismic waves recorded at the bottom floor has been in the order of 100 gal at the highest. Mostly, it is below 20 gal.

Among the wave forms obtained, 436 components of 45 earthquakes, which are assumed to be fairly large, were selected and the maximum acceleration amplitude and the predominant period were directly read.

Furthermore, for records of larger values (maximum acceleration at the bottom floor is 20 gal and over), the acceleration values were read by digital tracer at 1/100 second intervals and converted to numerical data, and the analysis of response spectra and so forth was made.

4. NATURAL FREQUENCY OF BUILDINGS

Of the buildings in Fig. 2, 21 typical telephone exchanges, that are from 2 to 10 stories high and are RC or SRC construction, were chosen. Their primary natural vibration periods along two horizontal directions were estimated from the predominant periods gained from the records at the roof or the uppermost floor.

The relation between the natural period and the number of above-ground stories is shown in Fig. 3. The relation between the natural period with the total number of stories is presented in Fig. 4. The primary natural period for 2 ~ 10 story buildings may be said to lie approximately within the 0.2 ~ 0.7 second range. Figure 5 shows estimated natural period for telephone exchange buildings, induced from the usual microtremor. No conspicuous difference is observed, when compared with the period derived from the records of earthquakes.

Approximation formulas for the relation between the primary natural period and the number of stories are:

$$\text{From Fig. 3,} \quad T = 0.03 + 0.06 F \quad (1)$$

$$\text{From Fig. 4,} \quad T = 0.08 + 0.04 F' \quad (1)'$$

where T: Primary natural period of building, F: Number of aboveground stories, F': Total number of stories (including basement).

In order to compare with buildings for general use, estimated natural period for two office buildings are also plotted in Fig. 3. In spite of the difference in the floor height, their values are close to those for the telephone exchanges. From these data, the natural period for a common building and that for a telephone exchange building seem to be equivalent, through the number of aboveground stories.

5. ACCELERATION AMPLIFICATION RATIO ALONG THE VERTICAL DIRECTION IN THE BUILDING

With reference to the results of investigation on 21 buildings reported in the previous section, a distribution diagram for the maximum acceleration along the vertical direction is made by drawing straight lines through the plotted points of the maximum horizontal acceleration at the observation floors for each earthquake. However, for buildings that lack accelerograph installation at their first floor, in view of the fact that the records of the buildings fitted with the accelerographs on their first or second floor, the acceleration gradient below that floor is about 1/2 of the gradient above it. The acceleration gradient for the underground portion is modified to 1/2 of the gradient for the aboveground portion by shrinking the ordinate of the underground portion. In Fig. 6, the maximum acceleration distribution for each building at the time of the Izu-Hanto-Okii Earthquake is shown.

Next, the distributions are rearranged with respect to each building. Figure 7 shows one of the examples. The maximum acceleration distribution curve shape does not seem to vary widely with different earthquakes.

Then, with respect to the individual distribution, the acceleration amplification ratios at each floor are calculated by putting the value at the first floor as unity and their mean values are taken along two horizontal directions. The example of the change in values for the acceleration amplification ratio along the vertical direction within the building thus obtained is shown in Fig. 8.

Furthermore, taking into consideration the increase in the acceleration toward the higher floor and the practicability of handling

the data, the authors divided buildings into 4 groups which are the roof, the upper floors (the upper half of the aboveground floors), the lower floors (the lower half of the aboveground floors) and the floors below the first floor. The uppermost floor and the middle floor represent the upper floor group and the lower floor group, respectively. Then, the values at the roof, the uppermost floor, the middle floor and the first floor were observed. The relation between the number of aboveground floors for the building and the acceleration amplification ratios at the representative floors, obtained with respect to each building, are shown in Fig. 9.

The acceleration amplification ratios show fairly wide dispersion, depending upon the buildings. However, the upper limit of the acceleration amplification ratio versus the first floor is approximately deemed to be 2 times that at the middle floor, 3.2 times that at the uppermost floor and around 4 times that at the roof.

6. ACCELERATION RESPONSE SPECTRUM OF BUILDING FLOOR

Of the records obtained up to the present, 13 buildings are chosen in order of the acceleration response spectra were calculated for every observation floor and along two horizontal directions, 68 waves all told. The damping ratio is assumed to be 3%. Figure 10 shows an example of the response spectrum for each floor. The spectrum value is normalized for each floor. The response spectrum characteristics vary with each floor. Peaks are observed which are assumed to be generated due not only to the primary natural period of the building but also due to the ground condition of the secondary period of the building and so forth.

Then, the response spectra obtained for each building were superimposed in a diagram for each representative floor of four groups of floors mentioned in the previous section. The results are shown in Fig. 11. While the peak value in the response spectrum ranges over 5 ~ 9 times at any representing floor of every group, when the damping ratio is 3%, the diagram shows that the period, at which the peak occurs, widely scatters.

Furthermore, in order to determine the average features for the spectra in Fig. 11, the mean values and the standard deviations were calculated. The results are shown in Fig. 12. In all groups, the peak value of the average response multiple lies at around 3 ~ 4 times and occurs at a period of around 0.3 ~ 0.5 second. The standard deviation is known to be somewhat less than 40% of the mean value, as well.

At the same time, in order to determine the change in the response spectra, the response spectra, when the damping ratio is changed from 1% to 10%, are measured at 6 points in two representative buildings along two horizontal directions. One of the results is shown in Fig. 13. From the result, the response spectra when damping are 1%, 2%, 5% and 10% ratio to the 3% damping is known to be around 1.4, 1.15, 0.85 and 0.7 respectively, in the vicinity of the peak value. It is also known that the differences diminish in the range off the peak.

7. SEISMIC FORCE USED FOR DESIGNING APPENDAGE

From the results gained in the above, a calculation was investigated for determining seismic forces to be adopted when appendages to be attached to a building floor are designed.

The seismic forces can be represented by the following formula:

$$P = K_0 \cdot K_1 \cdot K_2 \cdot W \cdot I \quad (2)$$

where K_0 : Standard seismic coefficient (seismic coefficient: acceleration/acceleration of gravity), K_1 : Acceleration amplification ratio for building floor, K_2 : Acceleration response ratio for appendage, W : Weight of appendage, I : Importance factor

The acceleration amplification ratio for the building floor can be represented, as is shown in Table 1, if the highest value for each floor group is adopted from the result of the investigation reported in Section 5. The seismic coefficient for the building floors is shown in Table 1, when 0.25 is given as the standard coefficient.

With regard to the acceleration response ratio, the investigation was made, based upon the acceleration response spectra discussed in Section 6, with the assumption that the appendage has an elastically equivalent behavior and that its weight is small compared with that of the building. This discussion is made based upon the mean response spectra, as shown in Fig. 12, following the conventional method of determining the standard spectrum for the ground motion. When the seismic coefficient of the building floor is taken as the upper limit to be assumed, it would be reasonable to adopt the mean spectra. However, since the period range for the peak is $0.3 \sim 0.5$ second in these average spectra, the range was extended to $0.2 \sim 0.7$ second, considering the application to low height buildings or soft ground. If the result of study on the damping ratio is reflected in this data, the acceleration response ratio for the center of gravity for the appendage can be represented by Fig. 14.

The acceleration amplification ratio from the ground motion to the center of gravity for the equipment $K_1 \cdot K_2$ is going to be comprehensively discussed. Generally, for two statistically independent distributions I and II and the distribution of their product, there is the following relation, if their mean value and the standard deviation are put as (A_1, σ_1) , (A_2, σ_2) and (A_{12}, σ_{12}) respectively:

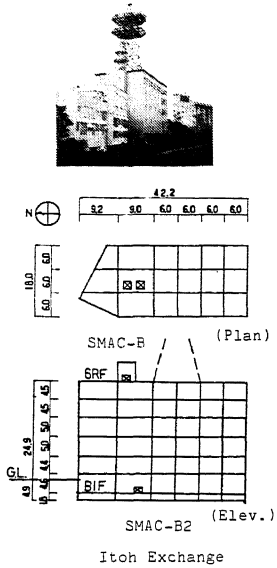
$$A_{12} = A_1 \cdot A_2 \quad \sigma_{12} = (A_1^2 \sigma_2^2 + A_2^2 \sigma_1^2 + \sigma_1^2 \sigma_2^2)^{1/2} \quad (3)$$

A case of an appendage on the roof, where damping ratio is 3%, is assumed. When the values in Fig. 9 ($A_1 = 2.48$, $\sigma_1 = 0.86$) and the peak values in Fig. 12 (a) are substituted in the above formula, $A_{12} = 7.68$ and $\sigma_{12} = 4.76$ are gained. From these results, it is determined that the value proposed by this report, $K_1 \cdot K_2 = 12$ mostly corresponds to $A_{12} + \sigma_{12} = 12.44$. That is, if the abovementioned calculation method is applied, in around 80% of the cases, including the cases in which the appendage response becomes very large, the value on the safe side could be given.

8. CONCLUSION

The authors rearranged the records obtained by the SMAC type strong-motion accelerographs, and proposed a calculation method for the seismic forces data used for designing the appendages to buildings, based upon these results.

If the energy absorbing potential of the appendage is taken into consideration, the accuracy of the seismic forces data to be assumed, especially when the appendage is about into the resonance range with the building, could be raised.



Itoh Exchange

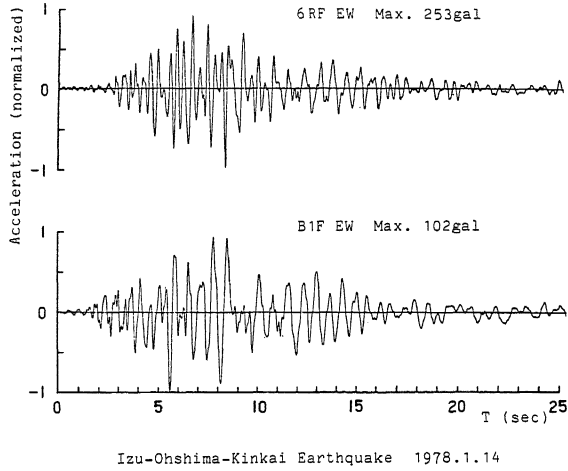


Fig. 1 Observed Records Example

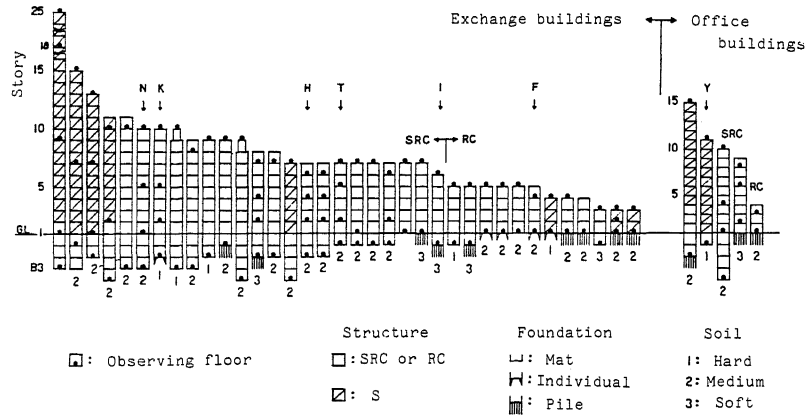


Fig. 2 Buildings where Earthquakes were Observed

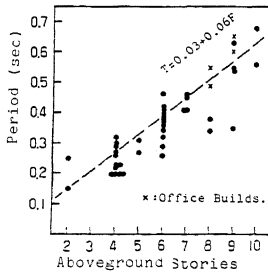


Fig.3 Natural Period vs. Aboveground Stories

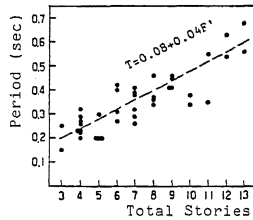


Fig.4 Natural Period vs. Total Stories

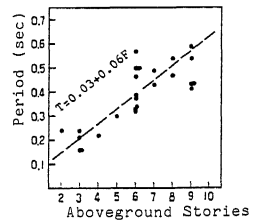


Fig.5 Natural Period induced from Microtremor vs. Aboveground Stories

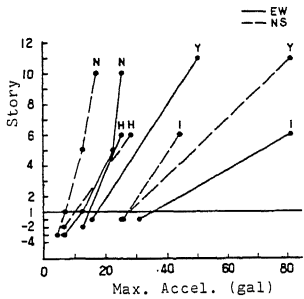


Fig. 6 Maximum Acceleration to Buildings during the Izu-Hanto-Oki Earthquake

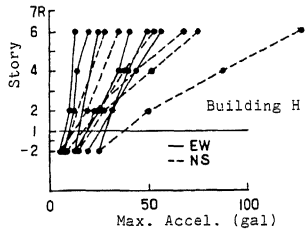


Fig. 7 Maximum Acceleration Distributions in Building

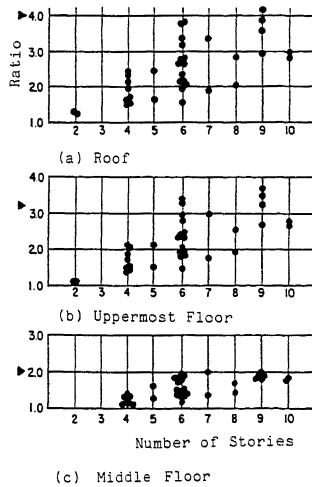


Fig. 9 Typical Floor Acceleration to First Floor Ratio

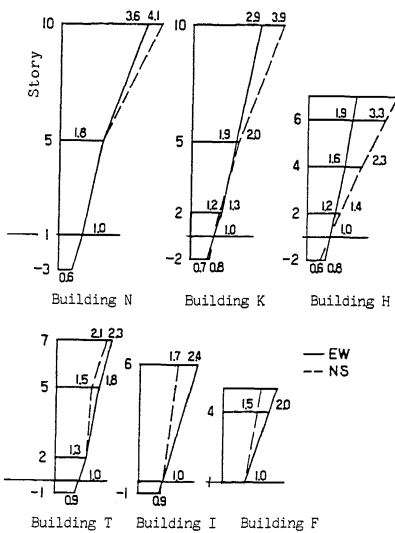


Fig. 8 Average Maximum Acceleration Distributions in each Building

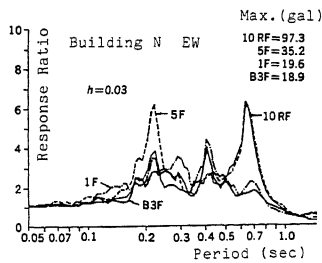


Fig. 10 Example of Floor Response Spectra in a Building

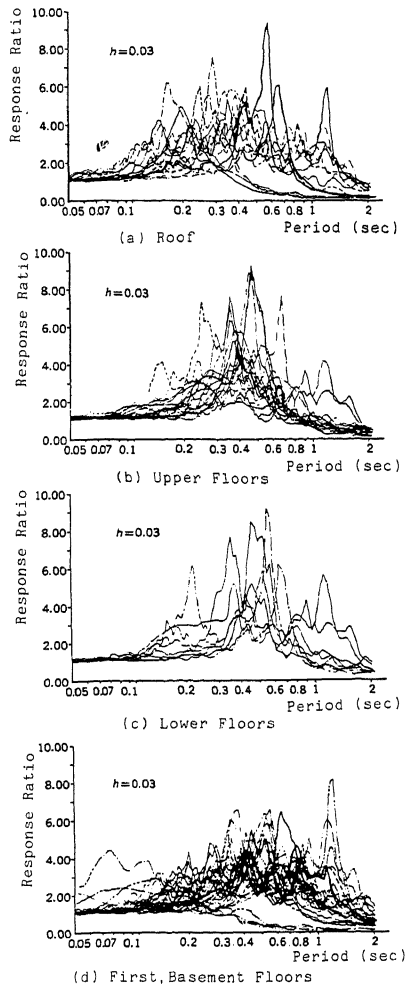


Fig.11 Response Spectra for each Floor Group

Table 1 Floor Acceleration Ratio

Floor	Ratio	Seismic Coef. (Example)
Roof	4.0	1.0
Upper	3.2	0.8
Lower	2.0	0.5
First Basement	1.0	0.25

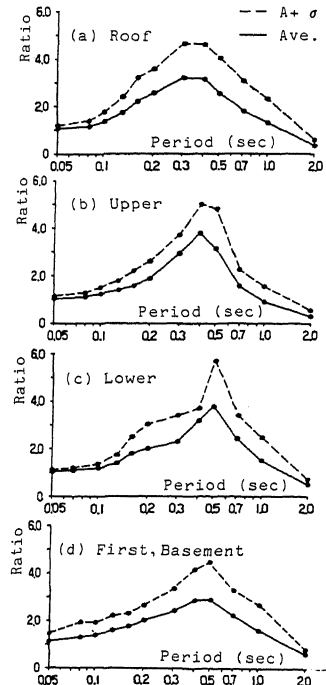


Fig.12 Mean Response Spectra for each Floor Group

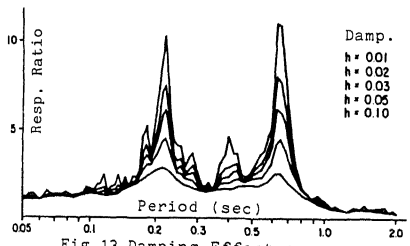


Fig.13 Damping Effect on Response Spectra

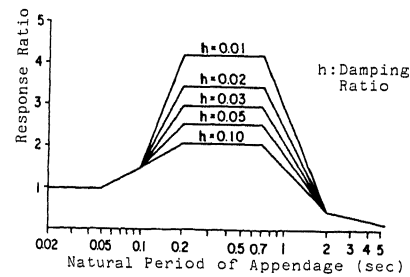


Fig.14 Appendage Gravity Center Acceleration Response Ratio